Sensitivity of Surface Ozone Simulation to Cumulus Parameterization

ZHINING TAO, ALLEN WILLIAMS, HO-CHUN HUANG,* MICHAEL CAUGHEY, AND XIN-ZHONG LIANG

Illinois State Water Survey, Champaign, Illinois

(Manuscript received 18 May 2007, in final form 3 October 2007)

ABSTRACT

Different cumulus schemes cause significant discrepancies in simulated precipitation, cloud cover, and temperature, which in turn lead to remarkable differences in simulated biogenic volatile organic compound (BVOC) emissions and surface ozone concentrations. As part of an effort to investigate the impact (and its uncertainty) of climate changes on U.S. air quality, this study evaluates the sensitivity of BVOC emissions and surface ozone concentrations to the Grell (GR) and Kain–Fritsch (KF) cumulus parameterizations. Overall, using the KF scheme yields less cloud cover, larger incident solar radiation, warmer surface temperature, and higher boundary layer height and hence generates more BVOC emissions than those using the GR scheme. As a result, the KF (versus GR) scheme produces more than 10 ppb of summer mean daily maximum 8-h ozone concentration over broad regions, resulting in a doubling of the number of high-ozone occurrences. The contributions of meteorological conditions versus BVOC emissions on regional ozone sensitivities to the choice of the cumulus scheme largely offset each other in the California and Texas regions, but the contrast in BVOC emissions dominates over that in the meteorological conditions for ozone differences in the Midwest and Northeast regions. The result demonstrates the necessity of considering the uncertainty of future ozone projections that are identified with alternative model physics configurations.

1. Introduction

The impact of climate changes on regional air quality has become a central topic in recent studies (e.g., Hogrefe et al. 2004; Langner et al. 2005; Murazaki and Hess 2006; Steiner et al. 2006). Climate changes affect regional air quality in two ways: 1) rising solar radiation and temperature enhance photochemical and chemical reaction rates and increase the emissions of biogenic volatile organic compounds (BVOC) that participate in the nitric oxide (NO_x)–VOC–ozone (O_3) cycle, which may lead to deterioration of local air quality (e.g., Chameides et al. 1988; Pierce et al. 1998; Tao et al. 2003); 2) changing wind circulation and planetary boundary layer structure directly alter air quality through dilution and advection (Hogrefe et al. 2004; Leung and Gustafson 2005).

For the purpose of studying climate change impacts on future air quality, a regional climate model (RCM) often is used to provide climate conditions at regional to local scales. The RCM is driven by lateral boundary conditions (LBCs) constructed from global general circulation model (GCM) simulations of the present and future climate (Liang et al. 2004a,b). These RCM meteorological conditions also determine the intensity of BVOC emissions, and together they provide essential inputs for air-quality model (AQM) simulation.

The RCM downscaling skill is sensitive to the selection of cumulus schemes and highly dependent upon weather or climate regimes (Liang et al. 2004a,b; Mapes et al. 2004; Zhu and Liang 2007). Studies have shown that different cumulus schemes lead to significant discrepancy in predictions of precipitation and temperature; although no single scheme performs equally well under all conditions (Wang and Seaman 1997; Giorgi and Shields 1999; Gochis et al. 2002). For example, Liang et al. (2004a) demonstrate that, in comparison with the observations, the Grell scheme (hereinafter referred to as GR; Grell 1993) produces better simulations of nocturnal precipitation maxima in the central United States and the associated eastward propagation of convective systems controlled by large-scale tropo-

* Current affiliation: Science Applications International Corporation, Camp Springs, Maryland.

Corresponding author address: Zhining Tao, Illinois State Water Survey, University of Illinois at Urbana–Champaign, 2204 Griffith Dr., Champaign, IL 61820.
E-mail: ztao@uiuc.edu

DOI: 10.1175/2007JAMC1780.1

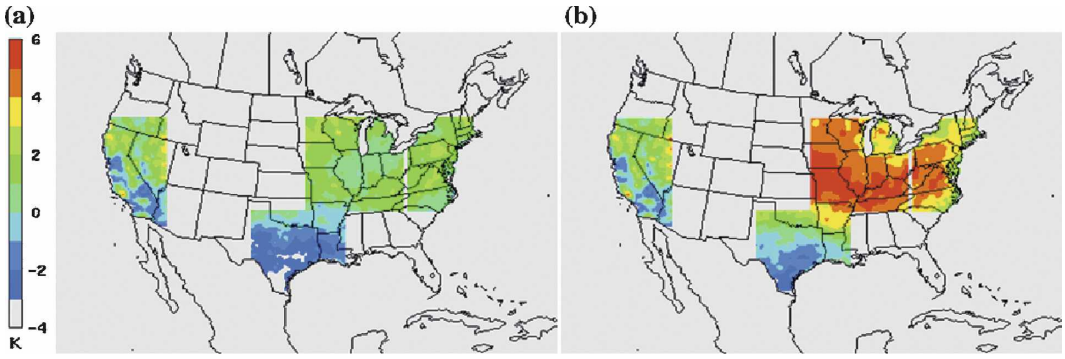

FIG. 1. Spatial distribution of differences in summer average surface temperature (simulation − observation): (a) RCM-GR and (b) RCM-KF.

spheric forcing, whereas the Kain–Fritsch scheme (hereinafter referred to as KF; Kain and Fritsch 1993) is better for the late afternoon peaks in the southeast United States where convection is governed by near-surface forcing. The results from Liang et al. (2004b) show that KF is superior to GR in simulating rainfall amount in the North American monsoon region, whereas in the southeast United States, KF overestimates rainfall amount but GR underestimates it.

The sensitivity of these meteorological parameters, for example, precipitation and temperature, to the choice of the cumulus scheme may lead to large differences in simulations of biogenic emissions and air quality. This motivates an explicit comparison of RCM simulations with different cumulus schemes and their influences on BVOC emissions and ambient O_3 concentration. The differences provide a measure of uncertainty in air-quality projections induced by the choice of the cumulus scheme. The effort is essential to better understand the overall uncertainty in air-quality modeling, to project a more credible range of regional air-quality changes under specific emissions and climate change scenarios, and consequently to formulate a more effective O_3 control strategy.

This study explores the impact of two widely used cumulus schemes—GR and KF—on RCM downscaling skill and the resultant changes in BVOC emissions and regional O_3 concentrations. Key meteorological parameters that impact BVOC emissions and O_3 formations are analyzed, and the sensitivity of O_3 concentrations to the choice of the two cumulus schemes is reported.

2. Model simulations

The modeling system includes an emissions model, an RCM, and an AQM. The RCM adopts a 30-km grid resolution over an extended U.S. domain. The AQM uses, respectively, 90- and 30-km grid spacing for the outer domain and four one-way nested inner subdomains (Fig. 1). The outer domain optimally integrates LBCs for the RCM simulation (Liang et al. 2001) and appropriately represents large-scale transport of air pollutants (Huang et al. 2007). The four nested subdomains are centered in California (CA), the Midwest (MW), the northeast United States (NE), and Texas (TX), respectively. They are designed to better resolve regional processes that govern local air quality. For AQM evaluation, nearly 4000 Air Quality System (http://www.epa.gov/ttn/airs/airsaqs/) monitoring stations are selected for direct comparison of modeled versus observed surface O_3 concentrations. Detailed analyses throughout the paper focus on 1998 summer (June–August) results for the four subdomains.

a. Regional climate model

The RCM is developed from the fifth-generation Pennsylvania State University–National Center for Atmospheric Research Mesoscale Model (MM5; Dudhia et al. 2004) with improvements to buffer-zone treatment, ocean interface, and cloud–radiation interactions as described in Liang et al. (2001, 2004b, 2006). Specifically, the planetary boundary layer is parameterized by the Medium-Range Forecast Model countergradient (nonlocal) turbulence transport scheme; solar and infrared radiation is estimated with the same scheme as in the National Center for Atmospheric Research Community Climate Model (CCM2) where the radiative effects of both cumulus and nonconvective clouds are taken into account; and the land surface process is modeled by the Oregon State University model.

The RCM employs a 23-level sigma coordinate with 30-km horizontal resolution. It provides meteorological inputs for both emissions estimates and chemical species transport and photochemical reactions of the AQM. The LBCs for the RCM are constructed from the global observational reanalysis (R-2) data by the

National Centers for Environmental Prediction–Department of Energy Atmospheric Model Intercomparison Project (AMIP-II) (Kanamitsu et al. 2002). Given that the R-2 represents one of the best proxies of the observed circulation, the RCM downscaling as driven by the R-2 LBCs provides the most realistic simulation of local–regional climate conditions (Liang et al. 2004a,b, 2006; Zhu and Liang 2005, 2007) such that the subsequent AQM results can be compared directly with the observations. With all other conditions identical, two RCM sensitivity experiments with the GR or KF cumulus scheme are conducted.

The GR scheme is a single-cloud model with updrafts and downdrafts and assumes quasi equilibrium in that clouds stabilize the environment at the same rate as the large-scale flows destabilize it; it does not represent entrainment or detrainment between clouds and environment (Grell 1993). In contrast, the KF scheme explicitly allows cloud–environment interactions; it uses a mass-conservative cloud model to represent entraining moist updraft and downdraft plumes and has a detailed representation of cloud physics (Kain and Fritsch 1993).

b. Emissions model (SMOKE)

The Sparse Matrix Operator Kernel Emissions modeling system (SMOKE) (Houyoux et al. 2000; Williams et al. 2001) is used to allocate emissions over a spatial grid, to simulate temporal resolution, and to split lumped inventory pollutants into various chemical species as required by the Regional Acid Deposition Model, version 2 (RADM2), chemical mechanism (Stockwell et al. 1990). Raw inventories applied in this study include the U.S. Environmental Protection Agency's (EPA) 1999 National Emissions Inventory (NEI99) (http://www.epa.gov/air/data) for the United States, the Big Bend Regional Aerosol and Visibility Observational (BRAVO) Study Emissions Inventory for the northern 10 states of Mexico (Kuhns et al. 2003; http://www.epa.gov/ttn/chief/net/mexico.html), and the National Pollutant Release Inventory (NPRI) for Canada (http://www.ec.gc.ca/pdb/npri).

The SMOKE incorporates the Biogenic Emissions Inventory System, version 2, (BEIS2) to calculate emissions from vegetation and soil. The algorithm used in BEIS2 is based on Guenther et al. (1995), which first calculates normalized biogenic emissions by multiplying land cover data with emissions factors, and then adjusts emissions according to temperature and solar radiation. The Biogenic Emissions Landcover Database, version 2, (BELD2) (Kinnee et al. 1997) is applied. BELD2 contains county-level (or equivalent) land cover data for the United States, Mexico, and Canada. These land cover data then are partitioned into each AQM grid cell using the ArcMap geographic information system. The RCM-GR and RCM-KF meteorological data are used to investigate the response of biogenic emissions to different cumulus schemes. As an integrated part of the ongoing EPA project to study the impacts of climate and emissions changes on U.S. air quality, we have continuously applied the BEIS2 to estimate BVOC. The latest version, BEIS3, incorporates the 1-km resolution BELD3 data with detailed land use categories (230 versus 127 in BEIS2), and may produce different BVOC emissions from BEIS2 (Yin et al. 2004). However, the purpose of this study is to reveal the sensitivity of BVOC emissions and subsequent O_3 concentrations to different meteorological inputs that result from the RCM downscaling with different cumulus parameterizations. The use of BEIS2 is sufficient and is not expected to change our key conclusions.

c. Regional Air-Quality Model

The AQM is developed from the San Joaquin Valley Air Quality Study/Atmospheric Utilities Signatures, Predictions, and Experiments study (SJVAQS/AUSPEX) Regional Modeling Adaptation Project (SARMAP) Air Quality Model (Chang et al. 1997), which improves the numerical scheme for solving gas-phase chemistry (Huang and Chang 2001). The AQM uses a terrain-following nonhydrostatic sigma coordinate system in the vertical direction with 15 layers. The depth of the lowest layer is approximately 77 m and a surface-layer submodel (SLS) that more realistically resolves the near-surface processes, for example, dry deposition, is applied to the lowest layer. The depth of the sublayer right above ground is about 15 m. The AQM calculates pollutant concentrations through simulations of physical and chemical mechanisms occurring in the atmosphere. Key meteorological parameters passed from the RCM to drive the AQM include temperature, pressure, wind, precipitation, and relative humidity (RH). The AQM rediagnoses clouds using the RH, temperature, and pressure information. The photolysis rates are obtained from a lookup table built within the AQM, and then corrected with cloud attenuation effects.

All AQM simulations conducted in this study utilize a one-way nesting approach and clean background chemical LBCs (Byun and Ching 1999) for the outer domain. A 3-day spinup is allowed to minimize impacts of initial conditions (Berge et al. 2001; Tao et al. 2003). More detailed information on the AQM can be found in Huang et al. (2007).

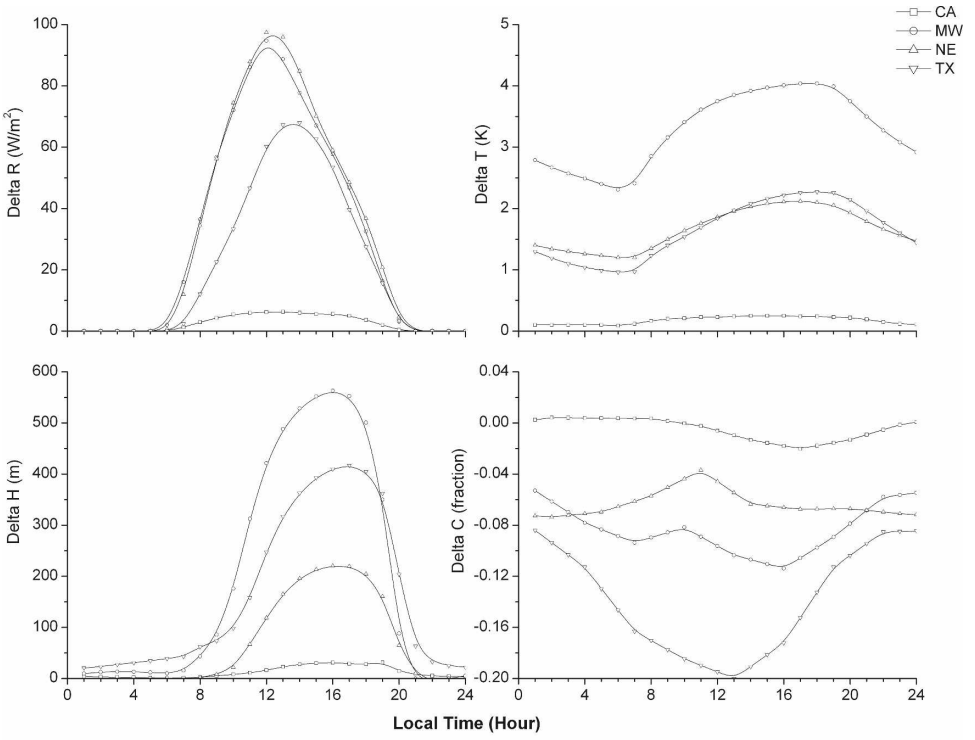

FIG. 2. The 1998 summer average diurnal differences of (top left) incident solar radiation (R), (top right) temperature (T), (bottom left) boundary layer height (H), and (bottom right) total cloud coverage (C) under RCM-GR and RCM-KF meteorology (difference = KF − GR) for the subdomains listed.

3. Results and discussion

a. RCM simulations

Figure 1 illustrates the RCM biases (differences from observations) of the 1998 summer mean surface temperature distribution over the four subdomains. Using either the GR or KF scheme, the RCM realistically reproduces surface temperature with biases less than 1 K in most CA. In MW and NE, the RCM simulation is reasonably good, having biases within 1 K in most areas using the GR scheme, but is significantly overestimated (>3 K) by the KF scheme. In TX, on the other hand, the RCM result using the KF scheme agrees well with the observations in a large portion of the subdomain, whereas that using the GR scheme produces underestimation (>2 K) almost everywhere. These results further depict that no single cumulus scheme is superior across a large region. The RCM surface temperature biases, averaged over CA, MW, NE, and TX, are +0.6, +1.1, +1.3, and −1.5 K, respectively, when using the GR scheme; and +0.8, +4.6, +3.6, and +0.3 K when using the KF scheme.

Figure 2 compares the diurnal differences in several meteorological parameters key to BVOC generation and surface O_3 formation, as simulated by the RCM, between using the GR and KF cumulus schemes. In general, the RCM using the KF scheme simulates less cloud cover, larger incident solar radiation, warmer surface temperature, and higher boundary layer height than those using the GR scheme. These parameters are interrelated. For example, the RCM-KF simulates less cloud cover, which can result in more intense incident solar radiation, and subsequently warmer temperature. Liang et al. (2006) discussed other reasons for the warmer surface temperature biases simulated using the KF scheme: 1) its tendency for a warmer and drier vertical heating profile near the cloud base, which would eventually affect surface temperature through turbulent mixing at the top of the planetary boundary layer; 2) its weaker low-level flow, which would allow more time for local surface heating to accumulate; and 3) its enhanced convective latent heating in the southeastern United States may produce a warmer air column over a broad region. The large differences between the results from the two cumulus schemes are anticipated to impose profound impacts on BVOC emissions and subsequent surface O_3 concentrations. This is the focus of the present study as discussed in the following sections.

TABLE 1. The 1998 summer mean biogenic emissions (tons day^{-1}) of isoprene and monoterpene based on the RCM-GR and RCM-KF meteorological output.

	Isoprene		Monoterpene	
Subdomain	RCM-GR	RCM-KF	RCM-GR	RCM-KF
California	5115	5251	3064	3121
Midwest	26 093	42 614	3608	5048
Northeast	16 457	24 971	4105	5228
Texas	18 088	25 233	5756	7077

b. Biogenic emissions

Table 1 compares the 1998 summer mean BVOC emissions in the four subdomains. Because the land cover data and emissions rates are prescribed, differences in the resulting BVOC emissions are caused solely by those in surface temperature and incident solar radiation simulated by the RCM using the GR versus KF cumulus scheme. Consistent with Fig. 2, BVOC emissions based on the RCM-KF meteorological output are larger than those based on the RCM-GR result. Figure 3 compares the differences in summer mean diurnal cycles of monoterpene and isoprene emissions based on the RCM meteorological data using the KF versus GR scheme. The difference is less than 3% between the two schemes for both monoterpene and isoprene in CA, while the RCM-KF meteorological results produces higher emissions in the other three subdomains. The RCM-KF meteorological output yields 23% higher monoterpene and 40% more isoprene in TX, 27% monoterpene and 52% isoprene in NE, and 40% monoterpene and 63% more isoprene in MW. The contrast of BVOC emissions between using the two meteorological simulations also displays large spatial variations in each subdomain (not shown). For example, in the isoprene-abundant regions [>150 tons day^{-1} (grid cell)$^{-1}$], emissions enhancement by the RCM using KF versus GR scheme is as large as 50%–70% in St Louis, Missouri, and adjacent areas, 40%–50% in eastern Virginia, and 30%–60% in Arkansas and northeastern Texas.

Temperature is the key parameter to determine BVOC emissions (Guenther et al. 1995). In CA, the summer mean temperature using the KF scheme is only 0.2 K higher than using the GR scheme, leading to insignificant changes in BVOC emissions. In NE and TX, the KF scheme produces warmer temperature with a diurnal range from 1 to 2.3 K, resulting in moderately larger BVOC emissions. The largest temperature increase from using the KF versus GR scheme is found in MW, with more than 3 K in the afternoon. As a result, the MW subdomain has the maximum increase in BVOC emissions. Incident solar radiation also plays an important role in biogenic isoprene generation (Guenther et al. 1995). A sensitivity study shows that the temperature differences account for more than 75% of total discrepancies in isoprene emissions in each of four subdomains, and the remaining 25% are attributed to the solar radiation differences.

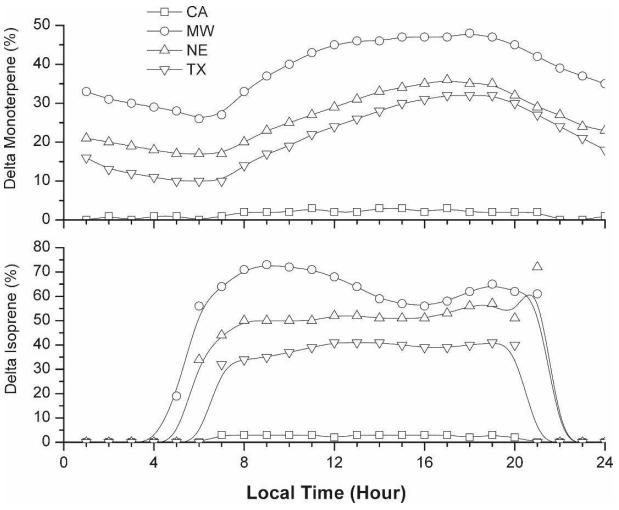

FIG. 3. The 1998 summer average diurnal differences of biogenic emissions of (top) monoterpene and (bottom) isoprene under RCM-GR and RCM-KF meteorological output [difference % = (KF − GR)/GR × 100%] for the subdomains listed.

c. Surface O_3 concentrations

1) COMPARISON WITH OBSERVATIONS

Hourly surface O_3 concentrations simulated by the AQM with emissions processed through SMOKE are compared with the AQS monitoring data. Both AQM and SMOKE are driven by the identical RCM meteorological output, either using the GR or KF cumulus scheme. For the comparison, any null values in the AQS database are eliminated. If there are multiple stations in a grid cell, the average concentrations are calculated and compared with the AQM result. Figure 4 shows the summer mean diurnal variations of surface O_3 concentrations averaged over each subdomain. Overall, the AQM simulation based on the RCM meteorological data using both GR and KF schemes catches the major characteristics of O_3 diurnal cycle. The phases of the modeled and measured O_3 match each other well but the magnitudes vary depending on regions. Among four subdomains, the AQM most realistically simulates O_3 concentrations in TX with little bias in daytime. In CA, the simulated O_3 cycles are almost identical between using two cumulus schemes mainly because the local precipitation is dominated by orographic forcing but not by convection (Liang et al.

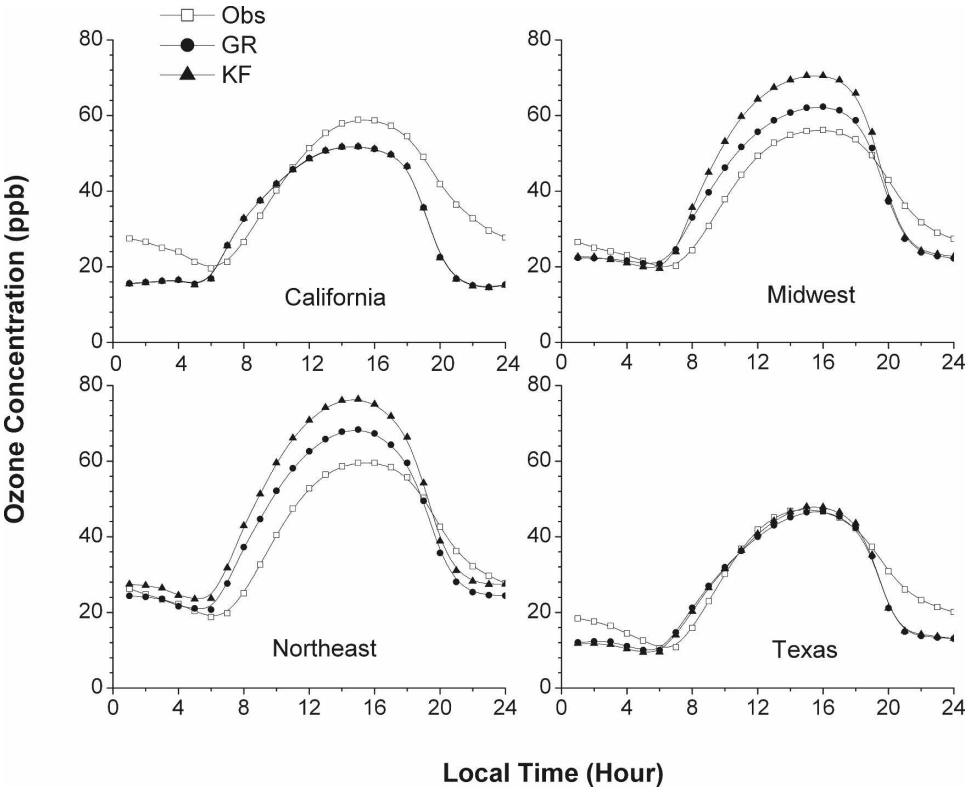

FIG. 4. The 1998 summer average diurnal variations in surface 1-h O_3 concentrations—observed and GR and KF cumulus schemes—in the four subdomains listed.

2004a). Both modeled values, however, are approximately 7% lower than observations averaged over the daytime hours. In the MW and NE subdomains, in contrast, the O_3 simulation is very sensitive to the choice of the cumulus scheme. In the daytime, on average, the simulated O_3 concentrations are higher than observations by 15% in MW and 19% in NE when using the RCM-GR meteorological output, while the respective O_3 concentrations are 30% and 35% higher when using the KF scheme. Liang et al. (2004a,b) demonstrated that the RCM with the GR scheme had higher skill than the KF scheme in simulating precipitation over these two regions.

Two statistical measures (Tesche et al. 1990)—normalized bias (NB) and normalized gross error (NGE)—are applied to further assess the model performance. This is based on the paired observation–simulation comparisons in 552 grids. There are 127, 202, 174, and 49 grid cells in the CA, MW, NE, and TX subdomains, respectively. Table 2 summarizes the domain-averaged results. In CA, the AQM, using the meteorological output with both cumulus schemes, underestimates surface O_3 concentration, having NB of approximately 13% and NGE of around 25%. In TX, the average NB is approximately −11% (underestimate) with NGE around 31% for both cumulus schemes. In

TABLE 2. Comparison of modeled surface O_3 concentrations with observations in the four subdomains.*

Subdomain	No. of observations**	NB (%)		NGE (%)	
		RCM-GR	RCM-KF	RCM-GR	RCM-KF
California	109 937	−13.3	−13.5	25.4	25.6
Midwest	179 247	6.1	20.4	29.8	36.8
Northeast	164 916	8.5	21.9	32.5	38.1
Texas	100 062	−11.7	−10.8	30.7	31.2

* Here NB = $(1/N)\Sigma_{i=1}^{N}(P_i - O_i)/O_i$; NGE = $(1/N)\Sigma_{i=1}^{N}(|P_i - O_i|)/O_i$; P and O are the modeled and observed 1-h average surface O_3 concentration, respectively; N is the number of observations.

** Only includes observed concentrations being greater than cutoff value of 40 ppb.

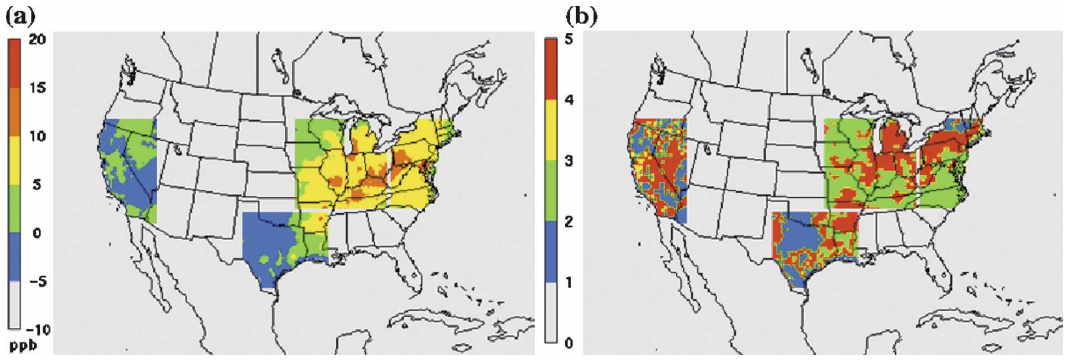

FIG. 5. Geographical distribution of (a) differences in the AQM-simulated 1998 summer average daily maximum 8-h O_3 concentrations based on RCM meteorological output using the KF vs GR cumulus schemes (difference = KF − GR) and (b) relative contributions to summer average daily maximum 8-h O_3 changes. Cases: 1 (blue) = MET dominant (>60%), 2 = EMS (green) dominant (>60%), 3 (yellow) = SYN dominant (>60%), and 4 (red) = combined.

MW, the AQM generally overestimates O_3 concentrations by about 6% and over 20% using the meteorological output with the GR and KF scheme, respectively. The corresponding NGE are approximately 30% and 37%. Similar to MW, the AQM overestimates O_3 concentrations in NE, with NB of 8.5% (RCM-GR) and 21.9% (RCM-KF), and the corresponding NGE are 32.5% and 38.1%.

The above results show that the AQM simulation of surface O_3 concentration is not sensitive to the cumulus parameterization in CA and TX. The sensitivity, however, is significantly larger in the MW and NE subdomains, where the AQM-simulated O_3 based on the RCM meteorological conditions using the GR scheme is more realistic than using the KF scheme. It is important to note that the relative performance of the GR versus KF scheme strongly depends on regions. This dependency is mainly determined by the RCM skill sensitivity, which is highly specific of distinct climate regimes (Liang et al. 2004a,b, 2006, 2007; Zhu and Liang 2007). There exists no single cumulus scheme that captures all physical processes governing convections over all regions. As such, it is currently most effective to use the ensemble RCM simulations with multiple cumulus schemes to more objectively evaluate the model skill in reproducing observations (Liang et al. 2006, 2007). For the same reason, it is desirable to study the sensitivity of air-quality modeling to the cumulus parameterization as a measure of result uncertainty.

2) INTERMODEL COMPARISON

Figure 5a illustrates the geographic distribution of differences in the 1998 summer mean daily maximum 8-h surface O_3 concentrations simulated by the AQM based on the RCM meteorological conditions using the KF versus GR cumulus schemes. Not surprisingly, the differences are very small (generally within 1 ppb) in CA because local meteorological conditions and BVOC emissions are very close between the two cumulus schemes (Figs. 2 and 3). In TX, differences are also small (±2 ppb) except in central Arkansas with relatively larger contrasts (up to 10 ppb). This latter region is identified with the largest increases in temperature (approximately 4 K) and isoprene emissions (about 60%) when replacing the GR with KF scheme. The largest differences in the average daily maximum 8-h O_3 concentrations occur in MW and NE, where local meteorological behavior and emissions responses to the choice of the cumulus scheme are strongest. In these two subdomains, the maximum 8-h O_3 concentration differences are typically 5–10 ppb, with more than 10 ppb in St. Louis, the Ohio River valley, and the coastal areas near Baltimore, Maryland, and over 30 ppb in the Washington, D.C. area. These large O_3 differences result mainly from the strong contrast of local meteorological behavior and BVOC emissions as discussed in the previous sections (Figs. 2 and 3). Noticeably, less cloud simulated by the RCM with the KF cumulus scheme leads to more intense solar radiation. Together with higher temperature, the RCM-KF meteorological output tends to result in more O_3 generation than the RCM-GR one.

Figure 6 compares the frequency distributions of 8-h O_3 concentration (>60 ppb) between using the KF and GR cumulus schemes. The difference is very small in CA, but significant over the other three subdomains, especially in MW, where high O_3 (>80 ppb) occurs more frequently when using the KF than GR scheme. The occurrences of high O_3 increase by a factor of 1.6,

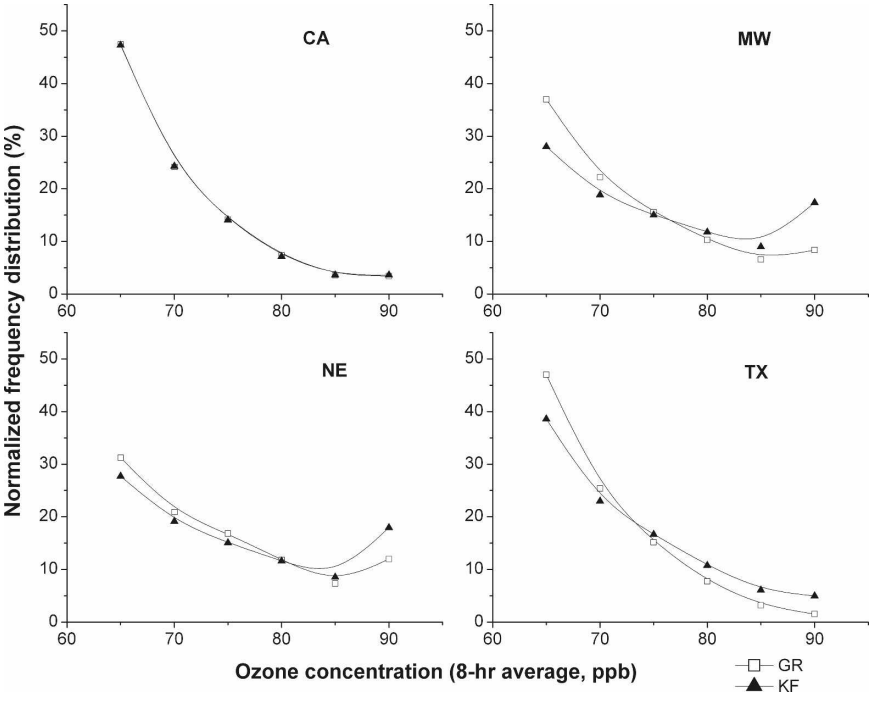

FIG. 6. Normalized frequency distribution of 1998 summer 8-h O_3 concentrations (>60 ppb) under RCM-GR and RCM-KF meteorological conditions in the four subdomains listed.

2.3, and 2.4 in NE, TX, and MW, respectively. This suggests that the probability of ambient standard violations increases when using the KF versus GR scheme in our modeling system to project future O_3 concentrations. The result implies the necessity of considering the uncertainty in the RCM meteorological outputs using different cumulus schemes when interpreting future O_3 responses to climate change scenarios.

d. Relative contributions to changes in surface O_3

Meteorological conditions affect surface O_3 concentrations by 1) determining photochemical–chemical reaction rates and horizontal–vertical transport—a direct effect—and 2) impacting biogenic emissions of O_3 precursor species and vertical distribution of inventory species—an indirect effect. As such, the total meteorological impact on surface O_3 concentrations using difference cumulus schemes can be separated into its direct or pure meteorological effect (hereinafter referred to as MET) without changing emissions, and its indirect or emissions effect (hereinafter referred to as EMS) due to emissions dependent on changing meteorological conditions.

These two effects, however, act simultaneously through complex nonlinear processes such that their contributions to the surface O_3 responses are not simply additive (Tao et al. 2003). Thus we define the synergistic effect (hereinafter referred to as SYN) to depict the contribution from the interaction between changing meteorological conditions and emissions. The SYN can be positive or negative as the interaction can increase or decrease the summation of the individual MET and EMS.

The factor-separation analysis (Stein and Alpert 1993) is used to estimate the MET, EMS, and SYN contributions to surface O_3 responses to the RCM meteorological output using GR and KF cumulus schemes. Four experiments (Table 3) were conducted. The first or base simulation uses RCM-GR emissions and RCM-GR meteorological output as AQM inputs (case 0); the second simulation uses RCM-GR emissions and RCM-KF meteorological output (case 1); the third simulation

TABLE 3. FSA experiment design.*

Case	Meteorological conditions	Emissions
0	RCM-GR	RCM-GR
1	RCM-KF	RCM-GR
2	RCM-GR	RCM-KF
3	RCM-KF	RCM-KF

* MET = case 1 − case 0; EMS = case 2 − case 0; SYN = case 3 − case 2 − case 1 + case 0.

uses RCM-KF emissions and RCM-GR meteorological output (case 2); and the fourth simulation uses RCM-KF emissions and RCM-KF meteorological output as inputs to the AQM (case 3). The difference between case 1 and case 0 is MET; the difference between case 2 and case 0 is EMS; and the difference between case 3 and case 0 is the sum of MET, EMS, and SYN. The relative contribution at each grid cell is calculated as

$$X\% = \frac{X}{|\mathrm{EMS}| + |\mathrm{MET}| + |\mathrm{SYN}|} \times 100\%,$$

where X is EMS, MET, or SYN. We identify the dominant factor if its contribution is greater than 60%.

Figure 5b displays the geographical distribution of the relative contributions of EMS, MET, and SYN to the responses of summer mean daily maximum 8-h O_3 concentrations to the RCM meteorological output using the KF versus GR schemes. In CA, the O_3 responses are not dominated by a particular factor but a result of the combined MET, EMS, and SYN contributions of similar magnitudes over most of the region, except in the southwestern corner of Arizona, southern Nevada, and spotted areas in California where MET dominates. In TX, MET dominates in the left portion (approximately 42% of the area) of the subdomain, whereas the EMS dominance scatters (about 14% of the area) to the right side, and all factors are equally important in the remaining areas. EMS is the dominant factor in the western and southern MW, as well as in the southern NE. Over most of these areas, biogenic emissions are abundant and temperature differences due to the choice of the cumulus scheme are large (Fig. 1), and hence the BVOC emissions differences due to the cumulus scheme change are significant, causing the EMS dominance.

Figure 7 displays the relative contributions averaged over each subdomain. MET contributes negatively to summer average daily maximum 8-h O_3 changes in CA and TX but positively in MW and NE. On average, SYN plays a negligible role in all four subdomains. On the other hand, EMS has large and positive contributions to surface O_3 sensitivity in all four subdomains, indicating the crucial role of biogenic emissions on regional O_3 formation. In projecting future O_3 change, misrepresentation of BVOC emissions may cause a large uncertainty.

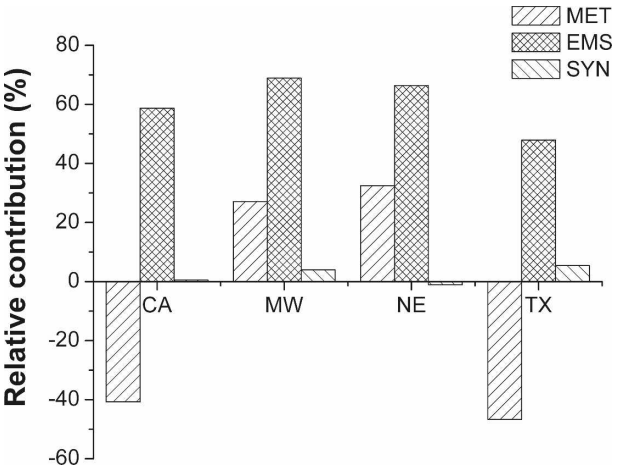

FIG. 7. Relative contributions (%) of emissions changes (EMS), meteorological changes (MET), and synergy (SYN) to differences in 1998 summer average daily maximum 8-h O_3 concentrations under RCM-GR and RCM-KF meteorological outputs.

4. Summary and conclusions

A comprehensive RCM–SMOKE–AQM system is applied to examine the impact of climate changes on U.S. air quality, focusing on four subdomains: CA, MW, NE, and TX. As part of an effort to evaluate the overall uncertainty of this modeling system in the impact study, we investigate the responses of BVOC emissions and surface O_3 concentrations to two cumulus schemes, GR and KF, used in the RCM. Results show that the RCM simulation is sensitive to the cumulus parameterization with strong regional dependence. While the RCM using both cumulus schemes shows a similar downscaling skill in CA, large discrepancies in the simulated meteorological conditions occur in MW, NE, and TX. The precipitation and surface temperature (Liang et al. 2004a,b; Zhu and Liang 2007) using the GR scheme agree better with observations in MW and NE, whereas those using the KF scheme are in better agreement with measurements in TX. This difference in the RCM meteorological output as the driving conditions profoundly affects the simulations of BVOC emissions and surface O_3 concentrations.

Changes in biogenic emissions is small (<3%) in CA because of the negligible RCM meteorological differences between using the GR and KF scheme. In TX, however, replacing the RCM meteorological output using the GR with KF scheme would result in increases of 23% in monoterpene and 40% in isoprene emissions. The respective increases in NE are 27% for monoterpene and 52% for isoprene. Among the four regions, the MW subdomain experiences the largest changes in BVOC emissions: 40% in monoterpene and 63% in isoprene.

In CA and TX, the AQM shows a similar skill to simulate regional O_3 concentrations using the RCM meteorological output with both GR and KF schemes. In MW and NE, however, warmer temperature simulated using the KF versus GR cumulus scheme leads to

higher surface O_3 concentrations. In MW, NE, and TX, the AQM-simulated occurrence of high O_3 (>80 ppb of 8-h average) driven by the RCM meteorological output approximately doubles when using the KF instead of GR cumulus scheme, indicating a large uncertainty in projecting future O_3 exceedance. The EMS, MET, and SYN effects all contribute to total O_3 changes, with both magnitude and sign varying among regions. The large EMS effect in all four subdomains indicates the important role of BVOC in regional O_3 formation.

Recently, the RCM community has begun to embrace the ensemble approach, in which a number of different physical representations are used in different regions of a domain with optimized weighting factors. For example, Liang et al. (2007) simulated the U.S.–Mexico summer precipitation using the ensemble of GR and KF cumulus schemes. The ensemble approach produced much more superior performances than each individual scheme over the entire study domain. In light of this, an ensemble method may reduce uncertainties in projecting future events and should merit more investigations.

The marked sensitivity of BVOC emissions and surface O_3 concentrations to the choice of the RCM cumulus parameterization found in this study poses a challenge on how to interpret future air quality. In light of this demonstration of the model sensitivity to cumulus schemes, the modeling community must consider the uncertainty associated with alternative model configurations in projecting future air-quality scenarios, based on which policy makers may integrate in their decisions a more realistic range of possible air-quality changes and impacts.

Acknowledgments. We acknowledge Forecast Systems Laboratory/National Oceanic and Atmospheric Administration and National Center for Supercomputing Applications/University of Illinois at Urbana–Champaign for the supercomputing support. The research was partially supported by the U.S. Environmental Protection Agency Science to Achieve Results (STAR) Awards RD-83096301-0 and R831449. The views expressed are those of the authors and do not necessarily reflect those of the sponsoring agencies or the Illinois State Water Survey.

REFERENCES

Berge, E., H.-C. Huang, J. Chang, and T.-H. Liu, 2001: A study of the importance of initial conditions for photochemical oxidant modeling. *J. Geophys. Res.,* **106,** 1347–1363.

Byun, D. W., and J. K. S. Ching, Eds., 1999: Science algorithms of the EPA Models-3 Community Multiscale Air Quality Model (CMAQ) modeling system. EPA/600/R-99/030, Office of Research and Development, U.S. Environmental Protection Agency, Washington, DC, 19 pp.

Chameides, W. L., R. Linsay, R. Richardson, and C. Kiang, 1988: The role of biogenic hydrocarbons in urban photochemical smog: Atlanta as a case study. *Science,* **241,** 1473–1475.

Chang, J. S., S. Jin, Y. Li, M. Beauharnois, C.-H. Lu, H.-C. Huang, S. Tanrikulu, and J. Damassa, 1997: The SARMAP Air Quality Model final report. Air Resource Board, California Environmental Protection Agency, Sacramento, CA, 82 pp.

Dudhia, J., D. Gill, Y.-R. Guo, K. Manning, W. Wang, and J. Chriszar, cited 2004: PSU/NCAR Mesoscale Modeling System tutorial class notes and user's guide: MM5 Modeling System Version 3. [Available online at http://www.mmm.ucar.edu/mm5/documents/MM5_tut_Web_notes/tutorialTOC.htm.]

Giorgi, F., and C. Shields, 1999: Tests of precipitation parameterizations available in latest version of NCAR regional climate model (RegCM) over continental United States. *J. Geophys. Res.,* **104,** 6353–6375.

Gochis, D. J., W. J. Shuttleworth, and Z.-L. Yang, 2002: Sensitivity of the modeled North America monsoon regional climate to convective parameterization. *Mon. Wea. Rev.,* **130,** 1282–1298.

Grell, G. A., 1993: Prognostic evaluation of assumptions used by cumulus parameterizations. *Mon. Wea. Rev.,* **121,** 764–787.

Guenther, A., and Coauthors, 1995: A global model of natural volatile organic compound emissions. *J. Geophys. Res.,* **100,** 8873–8892.

Hogrefe, C., and Coauthors, 2004: Simulating changes in regional air pollution over the eastern United States due to changes in global and regional climate and emissions. *J. Geophys. Res.,* **109,** D22301, doi:10.1029/2004JD004690.

Houyoux, M. R., J. M. Vukovich, C. J. Coats Jr., and N. J. M. Wheeler, 2000: Emission inventory development and processing for the seasonal model for regional air quality (SMRAQ) project. *J. Geophys. Res.,* **105,** 9079–9090.

Huang, H.-C., and J. S. Chang, 2001: On the performance of numerical solvers for chemistry submodel in three-dimensional air quality models. 1. Box-model simulations. *J. Geophys. Res.,* **106,** 20 175–20 188.

——, X.-Z. Liang, K. E. Kunkel, M. Caughey, and A. Williams, 2007: Seasonal simulation of tropospheric ozone over the Midwest and northeast United States: An application of a coupled regional climate and air quality modeling system. *J. Appl. Meteor. Climatol.,* **46,** 945–960.

Kain, J. S., and J. M. Fritsch, 1993: Convective parameterization in mesoscale models: The Kain–Fritsch scheme. *The Representation of Cumulus Convection in Numerical Models, Meteor. Monogr.,* No. 46, Amer. Meteor. Soc., 165–170.

Kanamitsu, M., W. Ebisuzaki, J. Woolen, S.-K. Yang, J. J. Hnilo, M. Fiorino, and G. L. Potter, 2002: The NCEP–DOE AMIP-II reanalysis (R-2). *Bull. Amer. Meteor. Soc.,* **83,** 1631–1643.

Kinnee, E., C. Geron, and T. Pierce, 1997: United States land use inventory for estimating biogenic ozone precursor emissions. *Ecol. Appl.,* **7,** 46–58.

Kuhns, H., M. Green, and V. Etyemezian, 2003: Big Bend Regional Aerosol and Visibility Observational (BRAVO) study emissions inventory. Prepared for BRAVO Technical Steering Committee, Desert Research Institute, Las Vegas, NV, 55 pp.

Langner, J., R. Bergstrom, and V. Poltescu, 2005: Impact of climate change on surface ozone and deposition of sulphur and nitrogen in Europe. *Atmos. Environ.,* **39,** 1129–1141.

Leung, L. R., and W. I. Gustafson Jr., 2005: Potential regional climate change and implications to U.S. air quality. *Geophys. Res. Lett.,* **32,** L16711, doi:10.1029/2005GL022911.

Liang, X.-Z., K. E. Kunkel, and A. N. Samel, 2001: Development of a regional climate model for U.S. Midwest application. Part I: Sensitivity to buffer zone treatment. *J. Climate,* **14,** 4363–4378.

——, L. Li, A. Dai, and K. E. Kunkel, 2004a: Regional climate model simulation of summer precipitation diurnal cycle over the United States. *Geophys. Res. Lett.,* **31,** L24208, doi:10.1029/2004GL021054.

——, ——, K. E. Kunkel, M. Ting, and J. X. L. Wang, 2004b: Regional climate model simulation of U.S. precipitation during 1982–2002. Part I: Annual cycle. *J. Climate,* **17,** 3510–3529.

——, J. Pan, J. Zhu, K. E. Kunkel, J. X.-L. Wang, and A. Dai, 2006: Regional climate model downscaling of the U.S. summer climate and future change. *J. Geophys. Res.,* **111,** D10108, doi:10.1029/2005JD006685.

——, M. Xu, K. E. Kunkel, G. A. Grell, and J. Kain, 2007: Regional climate model simulation of U.S.–Mexico summer precipitation using the optimal ensemble of two cumulus parameterizations. *J. Climate,* **20,** 5201–5207.

Mapes, B. E., T. T. Warner, M. Xu, and D. J. Gochis, 2004: Comparison of cumulus parameterizations and entrainment using domain-mean wind divergence in a regional model. *J. Atmos. Sci.,* **61,** 1284–1295.

Murazaki, K., and P. Hess, 2006: How does climate change contribute to surface ozone change over the United States? *J. Geophys. Res.,* **111,** D05301, doi:10.1029/2005JD005873.

Pierce, T., C. Geron, L. Bender, R. Dennis, G. Tonnesen, and A. Guenther, 1998: Influence of increased isoprene emissions on regional ozone modeling. *J. Geophys. Res.,* **103,** 25 611–25 629.

Stein, U., and P. Alpert, 1993: Factor separation in numerical simulations. *J. Atmos. Sci.,* **50,** 2107–2115.

Steiner, A. L., S. Tonse, R. C. Cohen, A. H. Goldstein, and R. A. Harley, 2006: Influence of future climate and emissions on regional air quality in California. *J. Geophys. Res.,* **111,** D18303, doi:10.1029/2005JD006935.

Stockwell, W. R., P. Middleton, J. S. Chang, and X. Tang, 1990: The second generation Regional Acid Deposition Model chemical mechanism for regional air quality modeling. *J. Geophys. Res.,* **95,** 16 343–16 367.

Tao, Z., S. Larson, D. J. Wuebbles, A. Williams, and M. Caughey, 2003: A seasonal simulation of biogenic contributions to ground-level ozone over the continental United States. *J. Geophys. Res.,* **108,** 4404, doi:10.1029/2002JD002945.

Tesche, T. W., P. Georgopoulos, J. H. Seinfeld, G. Cass, F. L. Lurmann, and P. M. Roth, 1990: Improvement of procedures for evaluating photochemical models. Report prepared by Radian Corporation for the State of California Air Resources Board, Sacramento, CA, 176 pp.

Wang, W., and N. L. Seaman, 1997: A comparison study of convective parameterization schemes in a mesoscale model. *Mon. Wea. Rev.,* **125,** 252–278.

Williams, A., M. Caughey, H.-C. Huang, X.-Z. Liang, K. Kunkel, Z. Tao, S. Larson, and D. Wuebbles, 2001: Comparison of emissions processing by EMS95 and SMOKE over the Midwestern U.S. *Tenth Int. Emission Inventory Conf.: One Atmosphere, One Inventory, Many Challenges,* Denver, CO, Environmental Protection Agency, 13 pp. [Available online at http://www.epa.gov/ttn/chief/conference/ei10/modeling/williams.pdf.]

Yin, D. Z., W. M. Jiang, H. Roth, and E. Giroux, 2004: Improvement of biogenic emissions estimation in the Canadian Lower Fraser Valley and its impact on particulate matter modeling results. *Atmos. Environ.,* **38,** 507–521.

Zhu, J., and X.-Z. Liang, 2005: Regional climate model simulation of U.S. soil temperature and moisture during 1982–2002. *J. Geophys. Res.,* **110,** D24110, doi:10.1029/2005JD006472.

——, and ——, 2007: Regional climate model simulations of U.S. precipitation and surface air temperature during 1982–2002: Interannual variation. *J. Climate,* **20,** 218–232.